

Baryon Rapidity Loss in Relativistic Au+Au Collisions

B.B. Back,¹ R.R. Betts,^{1,5} J. Chang,³ W.C. Chang,³ C.Y. Chi,⁴ Y.Y. Chu,² J.B. Cumming,² J.C. Dunlop,⁷ W. Eldredge,³ S.Y. Fung,³ R. Ganz,⁵ E. Garcia,⁶ A. Gillitzer,¹ G. Heintzelman,⁷ W.F. Henning,¹ D.J. Hofman,^{1,5} B. Holzman,⁵ J.H. Kang,⁹ E.J. Kim,⁹ S.Y. Kim,⁹ Y. Kwon,⁹ D. McLeod,⁵ A.C. Mignerey,⁶ M. Moulson,⁴ V. Nanal,^{1,5} C.A. Ogilvie,⁷ R. Pak,⁸ A. Ruangma,⁶ D.E. Russ,⁶ R.K. Seto,³ P.J. Stankas,⁶ G.S.F. Stephans,⁷ H.Q. Wang,³ F.L.H. Wolfs,⁸ A.H. Wuosmaa,¹ H. Xiang,³ G.H. Xu,³ H.B. Yao,⁷ and C.M. Zou³
(E917 Collaboration)

¹Argonne National Laboratory, Argonne, IL 60439, USA

²Brookhaven National Laboratory, Upton, NY 11973, USA

³University of California, Riverside, CA 92521, USA

⁴Columbia University, Nevis Laboratories, Irvington, NY 10533, USA

⁵University of Illinois at Chicago, Chicago, IL 60607, USA

⁶University of Maryland, College Park, MD 20742, USA

⁷Massachusetts Institute of Technology, Cambridge, MA 02139, USA

⁸University of Rochester, Rochester, NY 14627, USA

⁹Yonsei University, Seoul 120-749, South Korea

An excitation function of proton rapidity distributions for different centralities is reported from AGS Experiment E917 for Au+Au collisions at 6, 8, and 10.8 GeV/nucleon. The rapidity distributions from peripheral collisions have a valley at mid-rapidity which smoothly change to distributions that display a broad peak at mid-rapidity for central collisions. The mean rapidity loss increases with increasing beam energy, whereas the fraction of protons consistent with isotropic emission from a stationary source at midrapidity decreases with increasing beam energy. The data suggest that the stopping is substantially less than complete at these energies.

PACS number(s): 25.75.-q, 13.85.Ni, 21.65.+f

Nuclear matter is believed to be compressed to high baryon density (ρ_B) during central collisions of heavy nuclei at relativistic energies [1–3]. In the interaction region of the colliding nuclei, nucleons undergo collisions which reduce their original longitudinal momentum. This loss of rapidity is an important characteristic of the reaction mechanism, and is often referred to as stopping [4]. The rapidity loss for beam nucleons has been extensively studied in p+A reactions [5] and more recently in heavy-ion reactions [6–10]. Relativistic heavy-ion collisions are unique in the sense that secondary collisions of excited baryons are expected to contribute to the rapidity loss leading to simultaneous stopping of many nucleons within the interaction volume. The ρ_B thus reached may be large enough to induce phase transitions, such as quark deconfinement and/or chiral symmetry restoration [11]. The observation of large numbers of baryons at mid-rapidity is indicative of compression to high ρ_B , but the quantitative connection to ρ_B is only possible via model calculations. An important key to our understanding of this phenomenon is systematic data for the

rapidity distributions of baryons over a broad range of conditions, such as beam energy and centrality.

In this Letter, we present an excitation function of the centrality dependence of proton rapidity distributions from Au+Au collisions at 6, 8, and 10.8 GeV/nucleon. At these energies, the measured ratio of antiprotons to protons is very small ($< 0.03\%$) [12] and the production of protons from Λ decay contributes less than 5% to the total yield [13]. The measured protons can therefore be considered to directly reflect the distribution in rapidity of the initial baryons (assuming that the neutron rapidity distribution has a similar shape). The measured rapidity distributions at all three beam energies show a similar evolution with centrality. They are clearly bimodal in shape for peripheral collisions and change to shapes which for central collisions may still be bimodal in nature. This suggests that the degree of stopping in central collisions is not complete, even in this heavy system. In addition, it is shown that the protons do not end up as an isotropically emitting source at mid-rapidity, but retain a fair degree of their initial longitudinal motion. This phenomenon is represented by a parameterized fit to the data with a superposition of longitudinally moving sources.

Experiment E917 measured Au+Au reactions at beam kinetic energies of 6, 8, and 10.8 GeV/nucleon at the Brookhaven AGS, and was the final experiment in the series E802/E859/E866/E917 [14,15]. The experimental apparatus in E917 consisted of a series of beam-line detector arrays which were used for global event characterization, and a large rotatable magnetic spectrometer used to track and identify particles. The tracking system of the spectrometer consisted of a series of drift and multi-wire ionization chambers, which bracketed either side of a dipole magnet, followed by a segmented time-of-flight wall of vertical scintillator slats. The data presented here were taken with a trigger that required at least one track in the spectrometer. The centrality of an

event can be selected through either of two approximately equivalent methods: (1) from the multiplicity measured by a large acceptance device called the New Multiplicity Array [16], or (2) from the energy deposited in the zero degree calorimeter [16]. The data were sorted off-line into different centrality classes, where normalization was provided by prescaled interaction triggers. For each beam energy, the five event classes are reported as the percentage of the total interaction cross section ($\sigma_{\text{int}} = 6.8$ b), corresponding to (0-5)%, (5-12)%, (12-23)%, (23-39)%, and (39-81)% ((39-77)% for 10.8 GeV/nucleon) of σ_{int} .

The systematic uncertainty on the normalization of the measured invariant spectra and rapidity distributions is dominated by the uncertainty of the single-track efficiency and the loss of tracks due to hit-blocking. The tracking uncertainty increases from 5% to 10% towards mid-rapidity. For peripheral collisions, there is a 10% uncertainty in the cross section, which decreases to 5% for central collisions. These uncertainties lead to a total systematic uncertainty of 15% independent of centrality, with a 5% relative uncertainty across beam energies.

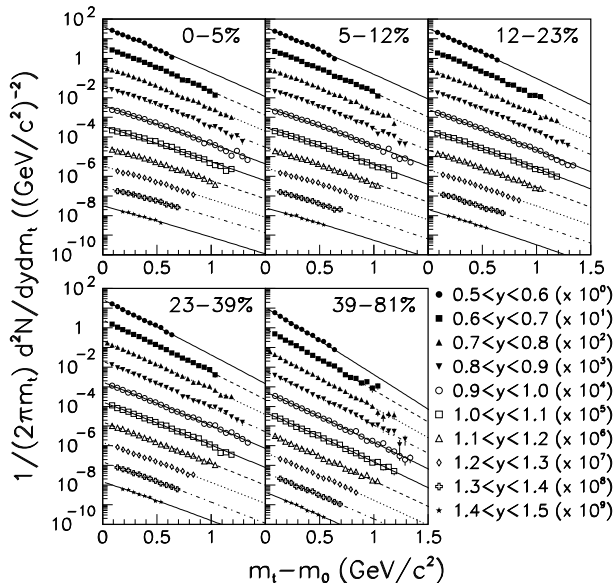


FIG. 1. Invariant yields of protons as a function of transverse mass for ten rapidity intervals for each centrality class of Au+Au collisions at 8 GeV/nucleon. The most backward rapidity in each panel is plotted on the correct scale, while successive spectra have been divided by ten for clarity. The errors are statistical only. The curves are Boltzmann fits described in the text.

The measured invariant yields of protons from Au+Au collisions at 8 GeV/nucleon are shown in ten rapidity intervals in Fig. 1 as a function of the transverse mass, $m_t = \sqrt{p_t^2 + m_0^2}$. The spectra at 8 GeV/nucleon are representative of the quality of the data at other beam energies. The errors are statistical only. The data were fit with a Boltzmann-form function in m_t :

$$\frac{1}{2\pi m_t} \frac{d^2N}{dm_t dy} = \frac{dN/dy}{2\pi(m_0^2 T + 2m_0 T^2 + 2T^3)} m_t e^{-(m_t - m_0)/T} \quad (1)$$

where T and dN/dy are free parameters. The data points were weighted according to their statistical errors. As has been previously reported, for Au+Au collisions at 10.8 GeV/nucleon [3], the proton spectra cannot be satisfactorily described by a single exponential function. In contrast, the above form reproduces the spectra well with χ^2 per d.o.f in the range 0.5 - 2.0, and provides the inverse slope parameter (T) and the rapidity density (dN/dy) for each rapidity interval.

The centrality dependence of the rapidity density at each beam energy is shown in Fig. 2. The data are shown relative to the rapidity of the center-of-mass of the system (y_{cm}) which equals 1.35, 1.47, and 1.61 for beam kinetic energies of 6, 8, and 10.8 GeV/nucleon, respectively. The data points reflected about mid-rapidity are shown as open symbols. The errors were calculated from the fitting procedure. The present values of dN/dy for the most central event class at 10.8 GeV/nucleon are in good agreement with the previously reported values from the E866 Collaboration [3].

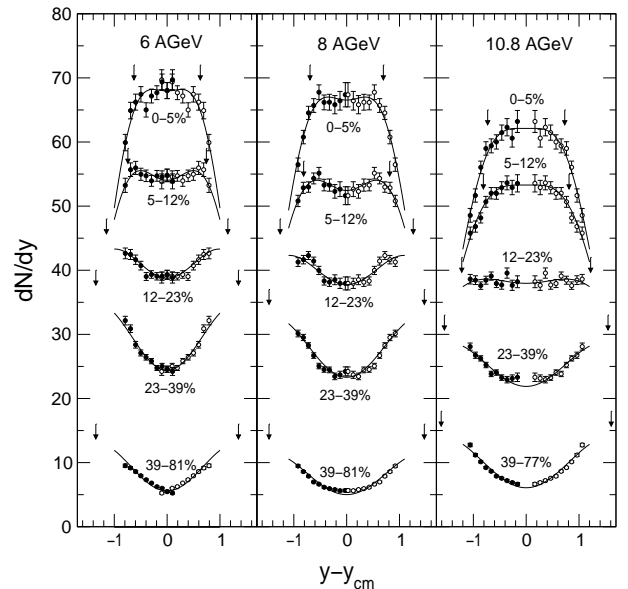


FIG. 2. Proton rapidity distributions for all centrality classes at all three beam energies from Boltzmann fits to the invariant cross sections. The open symbols are the data reflected about mid-rapidity. The errors are statistical only. The curves represent double Gaussian fits to the data (see text), the centroids of which are indicated by the arrows.

For each beam energy, a common trend is observed in the evolution of the shape of the rapidity distributions as a function of centrality. For the most peripheral event class the distribution has a minimum value of $dN/dy \approx 6$ at mid-rapidity. This concave shape persists to the next most central event class, corresponding to a centrality cut of (23-39)%, consistent with the expectation that most of the participant protons reside at beam rapidities follow-

ing these relatively peripheral collisions. For more central collisions, the rapidity distributions become progressively flatter, and begin to develop a broad maximum at mid-rapidity for all beam energies. The trend of the data suggests, however, that for the most central collisions, the distribution does not evolve to a single peak centered at mid-rapidity, but rather is consistent with two components each displaced from mid-rapidity, or with a set of sources spread throughout the rapidity range. To qualitatively emphasize this point, we have fit each of the measured distributions with two Gaussian peaks centered symmetrically about mid-rapidity. These are shown superimposed on the data for the three most central event classes at 8 GeV/nucleon in Fig. 3 and clearly display the trend. This result, somewhat surprisingly, implies that complete stopping is not achieved at AGS energies and that the longitudinal rapidity distribution is a result of transparency.

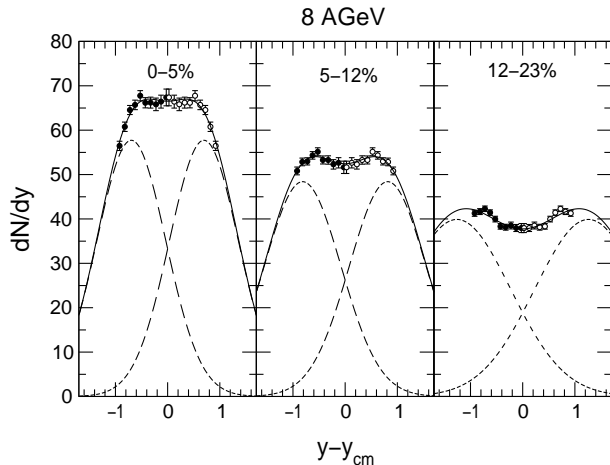


FIG. 3. Fits to the proton dN/dy distributions for the three most central event classes at 8 GeV/nucleon illustrating the evolution of shape with centrality. The solid curves are the sums of two individual Gaussians (dashed curves).

To quantify these results, we calculate the mean rapidity loss from the fits for the most central collisions $\langle \delta y \rangle = y_{beam} - \langle y \rangle$ where $\langle y \rangle$ refers to the Gaussians centered at positive rapidity. These values are listed in Table I. To compare with previous results for the most central data at 10.8 GeV/nucleon, we have also calculated the mean rapidity loss for protons in the restricted rapidity range $-1.11 < y - y_{cm} < 0$ and find a value of 1.07 ± 0.05 , which is in good agreement with the value of 1.02 ± 0.01 obtained for the (0-4)% most central Au+Au collisions at the same beam energy reported by Videbæk and Hansen [6].

The mean rapidity losses determined from our data show a systematic increase with incident energy. The mean rapidity loss does not, however, fully characterize all the features of the final rapidity distribution. Despite the fact that a considerable amount of the original longitudinal momentum of the incident particles has

been lost, the situation is clearly far from one where they are completely stopped. Fig. 4 shows the dN/dy distributions and inverse slopes for the (0-5)% most central event classes at all three energies plotted as solid points. The dashed curves in Fig. 4 show the expected distribution for complete stopping - *i.e.* isotropic emission from a source at rest in the center-of-mass system emitting protons with a Boltzmann energy distribution, the effective temperature of which is adjusted to reproduce the inverse slope of the transverse mass spectrum at mid-rapidity. The effective temperature thus accounts for the combined effects of radial expansion and temperature of this source.

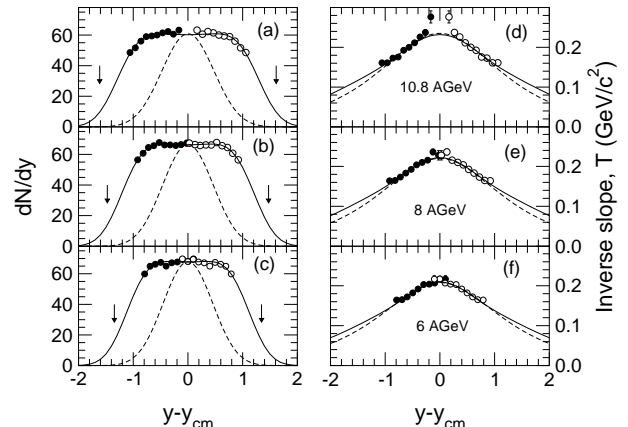


FIG. 4. Measured (solid points) and reflected (open circles) proton rapidity distributions and inverse slopes are shown as a function of rapidity $y - y_{cm}$ for beam energies of 6, 8, and 10.8 GeV/nucleon. The arrows indicate the target and beam rapidities. The dashed curves represent the expected distribution for isotropic emission from a thermal source at rest in the center-of-mass system ($y = y_{cm}$), whereas the solid curves correspond to an optimum fit to the data for a uniform distribution of sources within a range of rapidities $(y_{cm} - y_b) < y < (y_{cm} + y_b)$ with a Gaussian profile of $T_{eff}(y)$ centered at y_{cm} (see text). The parameters obtained from a least squares fit to the data are $y_b = 0.990, 1.086, 1.166$, $T_{eff}^0 = 0.253, 0.267, 0.279$ GeV/ c^2 , and $\sigma_T = 0.697, 0.762, 0.809$ for $E_{beam} = 6, 8, 10.8$ GeV/nucleon, respectively.

Whereas this gives a good description of the rapidity dependence of the inverse slope parameters, it completely fails for the dN/dy distributions. In fact, only a fraction of the observed yields can be accounted for in such a scenario. The yields can, however, be adequately accounted for by emission from a continuum of isotropic sources, uniformly distributed over a rapidity range $y_{cm} \pm y_b$. In order to account for the rapidity dependence of the inverse slope parameter it is, however, necessary to introduce a Gaussian rapidity dependency of the effective temperature $T_{eff}(y) = T_{eff}^0 \exp(-(y - y_{cm})^2 / 2\sigma_T^2)$. The solid curves shown in Fig. 4 were obtained by a four parameter simultaneous fit of y_b ; T_{eff}^0 ; σ_T ; and N_0 (dN/dy normalization) to the experimental dN/dy and inverse slope $T(y)$ values. Based on the fit dN/dy -distributions, the total

number of protons within the range $-2 < y - y_{cm} < 2$ ($\int_{-2}^2 \frac{dN}{dy} dy$) was found to be 155, 164, and 159 for $E_{beam} = 6, 8,$ and 10.8 GeV/nucleon, respectively. Since the total initial number of protons (158) is approximately accounted for, this suggests that the extrapolation into the unmeasured region is quite reasonable.

The fraction of the observed protons corresponding to complete stopping (f_{iso}) was calculated as the ratio of the areas under the dashed and solid curves, respectively. The values of f_{iso} at each energy are listed in Table I. The values of the absolute rapidity loss from the distributed source fits are also listed in Table I. They are in close agreement with the values from the Gaussian fits and show the same systematic increase with increasing incident energy. This result is different from observations in p+A collisions in which the rapidity loss was found to be independent of beam energy [5]. This would suggest an increased role of secondary interactions which increase stopping in heavy-ion collisions. In contrast, the fractional rapidity loss, $\langle \delta y \rangle / \delta y_{max}$, where $\delta y_{max} = y_{beam} - y_{cm}$, is found to be essentially constant with beam energy from 6 to 158 GeV/nucleon, similar to the trend noted in Ref. [7].

In summary and conclusion, we have measured proton rapidity distributions for Au+Au collisions at three energies as a function of collision centrality. These distributions show a consistent evolution with increasing energy and centrality leading to maximal rapidity loss for the most central collisions and the highest energy. This result suggests the importance of secondary reactions in the heavy-ion case, contrary to the situation in p+A collisions. Nevertheless, the degree of stopping of the incident baryons is far from complete and only a fraction of the observed protons can be accounted for by the emission from a stopped isotropically emitting source. The remainder still possess considerable longitudinal momentum. It is not possible to say unequivocally from the present data alone whether or not this corresponds to a situation where the colliding nuclei are, to some extent, “transparent”, or a fully stopped and compressed system has re-expanded. However, the systematic behavior of the centrality dependence of the shapes of the rapidity distributions suggests, surprisingly, that the former is the case.

This work is supported by the U.S. Department of Energy under contracts with ANL (No. W-31-109-ENG-38), BNL (No. DE-AC02-98CH10886), MIT (No. DE-AC02-76ER03069), UC Riverside (No. DE-FG03-86ER40271), UIC (No. DE-FG02-94ER40865), and the University of Maryland (No. DE-FG02-93ER40802), the National Science Foundation under contract with the University of Rochester (No. PHY-9722606), and the Ministry of Education and KOSEF (No. 951-0202-032-2) in Korea.

- [1] L. Ahle *et al.*, Nucl. Phys. **A590**, 249c (1995).
- [2] L. Ahle *et al.*, Nucl. Phys. **A610**, 139c (1996).
- [3] L. Ahle *et al.*, Phys. Rev. C **57**, R466 (1998).
- [4] W. Busza and A.S. Goldhaber, Phys. Lett. **B139**, 235 (1984).
- [5] W. Busza and R. Ledoux, Ann. Rev. Nucl. Part. Sci. **38**, 119 (1988).
- [6] F. Videbæk and O. Hansen, Phys. Rev. C **52**, 2684 (1995).
- [7] J.W. Harris, in *Advances in Nuclear Dynamics 2*, Eds. Bauer and Westfall, Plenum Press, NY, (1996).
- [8] B. Hong *et al.*, Phys. Rev. C **57**, 244 (1998).
- [9] H. Appelhäuser *et al.*, Phys. Rev. Lett. **82**, 2471 (1999).
- [10] J. Barrette *et al.*, Phys. Rev. C **62**, 024901 (2000).
- [11] E. Shuryak, Phys. Lett. **78B**, 150 (1978).
- [12] G. Heintzelman, Ph.D. thesis, MIT (1999).
- [13] W. Eldredge, Ph.D. thesis, UC Riverside (2000).
- [14] T. Abbott *et al.*, Nucl. Instrum. Meth. **A290**, 41 (1990).
- [15] L. Ahle *et al.*, Phys. Rev. C **58**, 3523 (1998).
- [16] L. Ahle *et al.*, Phys. Rev. C **59**, 2173 (1999).

TABLE I. Comparison between different measures of stopping in central heavy-ion collisions. The absolute $\langle \delta y \rangle$ and relative $\langle \delta y \rangle / \delta y_{max}$ rapidity losses obtained from double Gaussian fits to the dN/dy -distributions are given in column 2 and 3, respectively. The absolute and relative rapidity losses obtained from the fitted solid curves in Fig. 4(a-c) are given in column 4 and 5, respectively. Upper limits on the isotropic fraction f_{iso} of the total dN/dy distribution (solid curves in Fig. 4(a-c)) are given in column 6. The last row lists parameters obtained from an analysis of 158 AGeV Pb+Pb collisions at 0-5% centrality [9].

E_{beam} (AGeV)	Double Gaussian $\langle \delta y \rangle$	Distributed sources $\frac{\langle \delta y \rangle}{\delta y_{max}}$	Distributed sources $\langle \delta y \rangle^{(b)}$	Distributed sources $\frac{\langle \delta y \rangle}{\delta y_{max}}$	$f_{iso}^{(a)}$
6.0	0.72±0.01	0.53	0.74±0.01	0.55	0.49±0.01
8.0	0.78±0.01	0.53	0.82±0.01	0.56	0.46±0.01
10.8	0.88±0.01	0.55	0.93±0.01	0.57	0.45±0.01
158	1.71±0.02 ^(c)	0.59	-	-	0.23±0.02 ^(d)

^aFraction of isotropically emitted proton (dashed curves in Fig. 4(a-c)) of total number of protons (solid curves of Fig. 4(a-c)).

^bStatistical errors only.

^cObtained from a double Gaussian fit, $dN/dy = 85[\exp(-(y-y_{cm} + 1.19)^2/1.6) + \exp(-(y-y_{cm} - 1.19)^2/1.6)]$ to the experimental data [9].

^dObtained using $T_{iso} = 0.26$ GeV/ c^2 , which reproduces $\langle p_t \rangle$ at $y - y_{cm} = 0$ [9].